Pyrene-Derived Covalent Organic Framework Films: Advancements in Acid Vapor Detection

Shaikha Alneyadi * , Mohammed Alhassani , Ali Aleissaee , Ibrahim Al Mujaini

Posted Date: 27 December 2023

doi: 10.20944/preprints202312.2004.v1

Keywords: acid vapor; sensor; COF; pyrene; film

Article

Pyrene-Derived Covalent Organic Framework Films: Advancements in Acid Vapor Detection

Shaikha S. AlNeyadi *, Mohammed T. Alhassani, Ali S. Aleissaee and Ibrahim Al Mujaini

Department of Chemistry, College of Science, UAE University, Al-Ain 15551, United Arab Emirates
* Correspondence: shaikha.alneyadi@uaeu.ac.ae

Abstract: The expansion of global industries results in the release of harmful volatile acid vapors into the environment, posing a threat to various life forms. Hence, it's crucial to prioritize the development of swift sensing systems capable of monitoring these volatile acid vapors. This initiative holds great importance in safeguarding a clean and safe environment. This paper presents the synthesis and characterization of pyrene-based covalent organic frameworks (COFs) demonstrating exceptional crystallinity, thermal stability, and intense fluorescence. Three COFs—PP-COF, PT-COF, and PE-COF—were synthesized, showcasing large surface areas and robust thermal stability up to 400 °C. The fluorescence properties and intramolecular charge transfer within these COFs were significantly influenced by their Schiff base bonding types and π-stacking degrees between COF layers. Notably, PE-COF emerged as the most fluorescent among the three COFs and exhibited exceptional sensitivity and rapid response as a fluorescent chemosensor for detecting HCl in solution. The reversible protonation of imine bonds in these COFs allowed for the creation of highly sensitive acid vapor sensors, showcasing a shift in spectral absorption while maintaining structural integrity. This research highlights the potential of COFs as reliable and reusable sensors for detecting harmful acid vapors, addressing environmental concerns arising from industrial activities.

Keywords: acid vapor, sensor, COF, pyrene, film

1. Introduction

The impact of an individual's surroundings on their physical, mental, and social well-being cannot be overstated [1]. With the continuous evolution of human lifestyles, the environment has faced substantial alterations. Pollution of air, water, and soil has significantly affected daily life. Over the past decade, environmental degradation, especially due to air pollution, has been notably severe [2]. The atmosphere contains a multitude of air pollutants, including hazardous gases, toxic smokes, and dust, with hazardous gases posing the most significant threat. Exposure to these gases can result in various diseases such as cancer, chronic bronchitis, and even fatalities [2]. The detection of harmful gases holds immense importance due to their adverse effects on both the environment and human well-being. Among these noxious gases, hydrogen chloride (HCl) stands out as a level III hazardous airborne pollutant. Originating mainly from incineration plants, pharmaceutical, metallurgical sectors, chlorofluorocarbon (CFC) atmospheres, and accidental releases, gaseous HCl contributes significantly to acid rain formation and the generation of dioxins [3]. Exposure to HCl vapor has severe repercussions on both living organisms and the environment. It can cause damage to the mucosa of eyes and noses when surpassing recommended safety limits [4]. Inhalation of HCl vapor may lead to choking, coughing, and upper respiratory tract ulcers [5]. Additionally, it poses a threat to plants, leading to soil and water acidification. Organizations such as the Occupational Safety and Health Administration (OSHA) classify HCl as a workplace risk, defining a short-term exposure threshold of 5 ppm [5]. Incidents involving toxic HCl vapor leaks have been reported globally, including incidents in Frankfurt, Germany (December 2020), Lalru, Punjab (2015), and more recently in Hurstville Aquatic Leisure Centre, Sydney (April 2021), necessitating mass evacuations and

 doi:10.20944/preprints202312.2004.v1

hospitalizations due to adverse effects [6,7]. Thus, the development of a highly sensitive platform for detecting hazardous HCl vapor becomes imperative to monitor and avert accidental threats. In recent years, several approaches like optochemical, optical, gas chromatographic, and electrochemical sensors have been developed for detecting HCl vapor, each with its limitations such as time-consuming analysis, low sensitivity, and high cost [8]. Presently, there's a growing demand for improved sensing materials capable of detecting HCl with remarkable sensitivity, focusing on materials like metal oxides, lanthanide complexes, and conducting molecules, aiming for lower detection limits [9]. Among these, conducting materials draw significant attention due to their conductivity arising from conjugated π−π bonds, enabling their utilization in electrical and optical sensor devices [9]. Organic π-conjugated small molecules offer distinct advantages, including customizable structures, mechanical flexibility, and solution processability, making them promising candidates for cost-effective, portable gas sensors operable at room temperature. However, challenges persist in fabricating organic semiconductor gas sensors, including issues related to sensitivity, recovery, and response time [9,10]. Over the years, various sensor technologies have been developed to detect gaseous HCl, encompassing conductometric, amperometric, solid electrochemical, and optochemical sensors. However, these methods suffer from drawbacks such as prolonged response times, limited sensitivity, high operational costs, and safety concerns. In light of these challenges, there is an urgent need for the development of more accessible, efficient, rapid, and safer sensors capable of on-site detection to effectively identify the presence of HCl. This paper aims to contribute to this pressing need by introducing novel sensor materials based on ultrastable 2D COFs, offering promising prospects for enhanced and reliable HCl detection. Within the realm of crystalline polymers, covalent organic frameworks (COFs) have emerged as remarkable entities, characterized by their 2D or 3D periodic structures formed through reticular chemistry principles. These structures, constructed via covalent bonding of organic building blocks, exhibit exceptional attributes including high crystallinity, permanent porosity, substantial surface areas, and robust thermal stability [11]. Over the past decade, COFs have found diverse applications spanning catalysis, gas adsorption, separation, energy storage, medicine, optoelectronics, proton conduction, and chemical sensing due to their versatile covalent linkages—B–O, C–C, N–N, C–N, and B–N bonds—enabling tailored pore sizes, structures, and functionalities. While many COFs lack fluorescence or display weak emission, recent breakthroughs utilizing highly emissive or non-emissive building linkers, such as pyrene and hydrazone, have yielded highly fluorescent COFs [12]. These fluorescent COFs present distinct advantages over non-fluorescent counterparts. They offer faster response times, heightened sensitivity to environmental changes, superior physiochemical stability, and consistent monolithic pore sizes. Recent strides have seen the development of various fluorescent COFs serving as chemosensors for diverse analytes like mercury ions, pH variations, explosives like 2,4,6-trinitrophenol, electron-rich arenes, iron (III), and various anions. However, the landscape of COF-based chemosensors, particularly for detecting hydrogen chloride (HCl) gas, remains relatively unexplored [13]. In this study, we synthesized three highly stable 2D COFs—PP-COF, PT-COF, and PE-COF—showcasing remarkable Brunauer–Emmett–Teller (BET) surface areas of up to 1350 $m^2 g^{-1}$. These COFs were created through Schiff base formation in solvothermal conditions, employing 4,4',4'',4'''-(pyrene-1,3,6,8-tetrayl)tetraaniline and three distinct formyl species: 4,4',4''-(1,3,5-triazine-2,4,6-triyl)tribenzaldehyde, hexakis (4-aldehyde phenoxy) cyclotriphosphazene, and 4,4',4'',4'''-(ethane-1,1,2,2-tetrayl)tetra benzaldehyde, as illustrated in Scheme 1. Capitalizing on their substantial surface areas, exceptional stability, and strong fluorescence, these COFs demonstrated their capacity as sensitive chemosensors for detecting HCl. Among the COFs studied, PE-COF initially emits a faint yellow fluorescence. However, upon exposure to solid-state HCl gas, it rapidly transforms into a vibrant dark orange emission in less than a second. This swift and notable color shift is easily observable to the naked eye under regular visible light. Our paper aims to showcase an innovative system capable of detecting toxic acid vapors. Highlighting its ease of processing, cost-effectiveness, portability, and functionality in ambient conditions, we demonstrate its potential in constructing an electronic prototype for on-field

 doi:10.20944/preprints202312.2004.v1

applications. Our goal is to illustrate how this technology revolutionizes real-time monitoring of hazardous substances.

2. Results and Discussion

In this investigation, we capitalize on the distinctive electron configuration inherent in the imine linkages to serve as the defining functional constituent within a series of two-dimensional Covalent Organic Frameworks (COFs). These COFs are meticulously synthesized employing the 1,3,6,8-tetra(aminophenyl)pyrene (TAPA, as depicted in Scheme 1) as a foundational building block. Upon subjecting the imine bonds within these materials to protonation, our observations reveal a noteworthy red-shift in absorption, particularly in the near-infrared region, accompanied by the emergence of absorption bands induced by protonation. Importantly, these alterations manifest without compromising the structural integrity or crystalline attributes of the frameworks. We designed and created three COFs with outstanding stability and porosity by Schiff base reactions, as shown in Scheme 1. In the synthesis of pyrene-based covalent organic frameworks (COFs), the approach centered on employing 1,3,6,8-tetra(aminophenyl)pyrene (TAPA) as a pivotal 4-connected building block, serving as an amine linker. This strategic choice aimed to capitalize on TAPA's structural versatility. The coupling of TAPA with diverse compounds, including 4,4',4'',4'''-(ethane-1,1,2,2-tetrayl)tetra benzaldehyde (ETBA) (Scheme 1A), 4,4',4''-(1,3,5-Triazine-2,4,6-triyl)tribenzaldehyde (Scheme 1B), and hexa(4-formyl-phenoxy)cyclotriphosphazene (Scheme 1C). The synthesis process yielded three distinct two-dimensional (2D) structures termed PP-COF, PT-COF, and PE-COF. Detailed methods for synthesizing organic linkers, including reagents, reaction conditions, and purification techniques, are provided. The supporting data (Supplementary Materials, Section S2, Schemes S1–S3 and Section 3, Figures S1–S6) encompass comprehensive characterization techniques, such as spectroscopic analysis (e.g., NMR). The creation of the three targeted COFs utilized a solvothermal technique. Acetic acid served as a catalyst, and the building blocks were suspended in a solution comprising a mixture of (mesitylene/1,4-dioxane) or o-(dichlorobenzene/n-butanol). Subsequently, the compounds were subjected to solvothermal conditions at 120°C for 3-5 days (Supplementary Materials , Section S4). The successful creation of imine bonds was shown by the FT-IR spectroscopy study of PP-COF, PT-COF, and PE-COF, which showed strong stretching vibrations of the C=N unit in the range of 1622–1625 cm^{-1}. Further evidence of the success of the Schiff-base condensation process was provided by the spectra, which also revealed the removal of the N-H (3439-3398 cm^{-1}) stretching vibrations from the amino group in the amine linker and the C=O (1648-1660 cm^{-1}) vibration from the aldehyde linker (Supplementary Materials, Section S5, Figure S7). To examine the porous architectures of PP-COF, PT-COF, and PE-COF, nitrogen sorption isotherms at 77 K were employed (Figure 1A). Prior to the nitrogen sorption measurement, the COF samples underwent an overnight pre-treatment at 100°C in a vacuum. The nitrogen absorption of PP-COF, PT-COF, and PE-COF displayed rapid increments at lower pressures (P/P_o = 0 to 0.1), showcasing their microporous characteristics. The Brunauer-Emmett-Teller (BET) surface area measurements revealed values of 1350 $m^2 g^{-1}$, 1098 $m^2 g^{-1}$, and 730 $m^2 g^{-1}$ for PP-COF, PT-COF, and PE-COF, respectively. Evaluation of the total pore volumes at a P/P_0 ratio of 0.99 showcased a notable pore volume of 1.83 $cm^3 g^{-1}$ for PP-COF, surpassing both PT-COF (0.98 $cm^3 g^{-1}$) and PE-COF (1.23 $cm^3 g^{-1}$). Furthermore, nonlocal density functional theory (NLDFT) was employed to determine the pore sizes of the three COFs. The results unveiled pore sizes of 16 Å and 18 Å for PP-COF, and 12 Å and 17 Å for both PT-COF and PE-COF (Figure 1B).

Preprints (www.preprints.org) | NOT PEER-REVIEWED | Posted: 27 December 2023 doi:10.20944/preprints202312.2004.v1

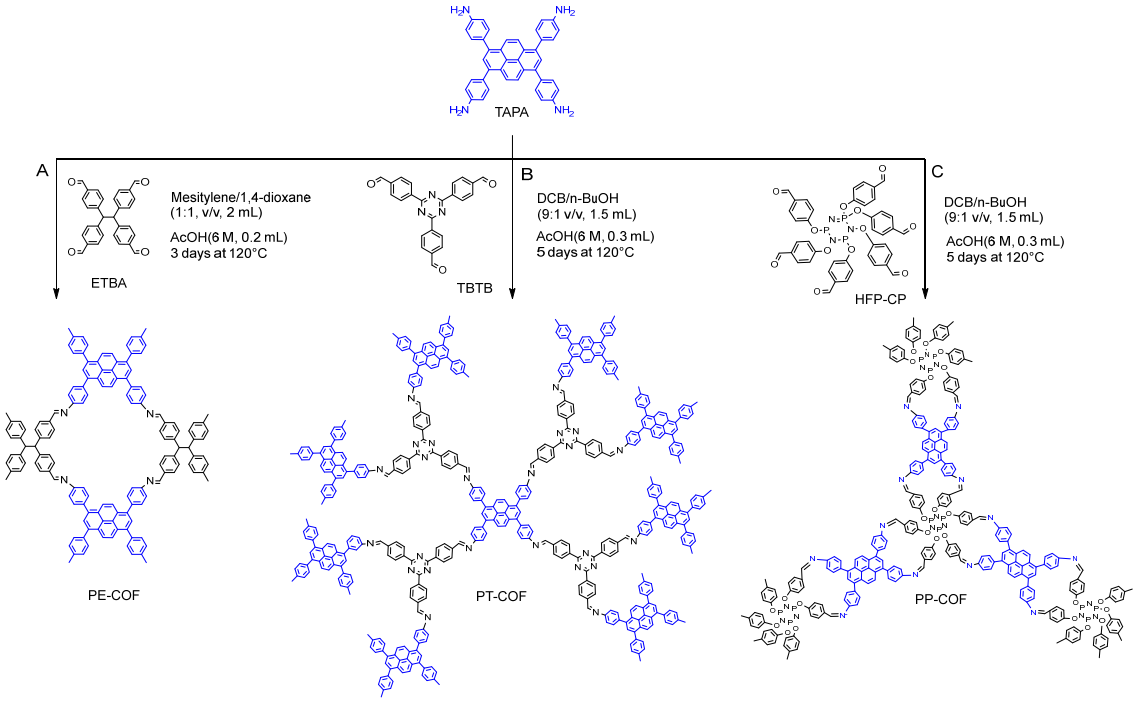

Scheme 1. Designing and Synthesizing PE-COF, PT-COF, and PP-COF.

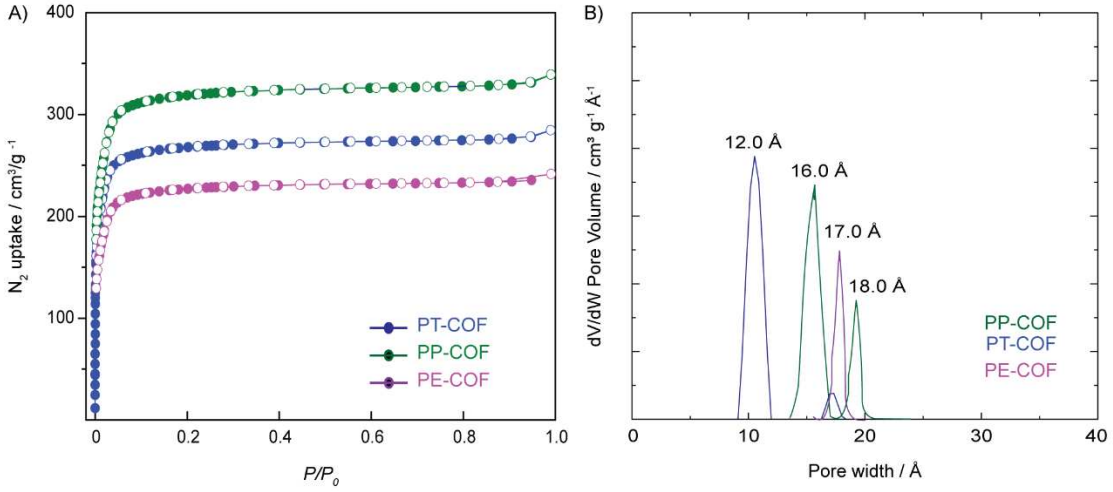

Figure 1. A) Nitrogen sorption isotherms of PP-COF, PT-COF, and PE-COF, at 77 K, with ● representing adsorption and ○ representing desorption; B) Pore size distributions of PP-COF, PT-COF, and PE-COF.

The crystalline characteristics of PP-COF, PT-COF, and PE-COF were investigated through powder X-ray diffraction (PXRD) analysis, as depicted in Figure 2. In the PXRD spectra of PT-COF (Figure 2A), distinct peaks corresponding to the 100, 110, 200, 210, 300, and 001 facets were observed at 3.98°, 5.06°, 9.34°, 11.68°, 14.85°, and 24.80°, respectively. Similarly, the PXRD pattern of PP-COF (Figure 2B) exhibited peaks at 2.68°, 5.58°, 9.82°, 12.54°, and 23.35°, attributed to the 110, 102, 200, 004, and 204 facets, respectively. In the case of PE-COF (Figure 2C), six distinctive peaks were identified, with the most intense peak at 5.56°, corresponding to the 100 facet, while others appeared at 6.78°, 7.31°, 9.52°, 11.67°, and 12.98°, representing the 110, 210, 220, 300, and 001 facets, respectively. To gain comprehensive insights into their structures, the PXRD patterns of the investigated COFs underwent simulation via the Pawley refinement technique. The simulated PXRD patterns (depicted by the red curve in Figure 2A–C) exhibited a close alignment with the experimental PXRD patterns (depicted by the black curve in Figure 2A–C). This agreement is evident from the difference pattern (indicated

Preprints (www.preprints.org) | NOT PEER-REVIEWED | Posted: 27 December 2023 doi:10.20944/preprints202312.2004.v1

by the green curve in Figure 2A–C), affirming the accuracy of the structural analysis. In the case of PT-COF (Figure 2A), the experimental PXRD pattern exhibited strong conformity with the simulated patterns derived from the AA-staggered stacking model, displaying favorable agreement factors (Rp = 1.33% and Rwp = 2.67%) with optimized parameters (a = b = 19.46 Å, c = 3.64 Å, $\alpha = \beta = 90°$, and $\gamma = 120°$). For PP-COF, the cell parameters were fine-tuned through Pawley refinements, showcasing minimal distinction between the experimental curve and simulated profiles produced by the AA-staggered stacking model (a = b = 30.17 Å, c = 3.43 Å, $\alpha = \beta = 90°$, and $\gamma = 120°$), yielding negligible residuals (Rp = 1.23% and Rwp = 3.27%) (Figure 2B). Moreover, the experimental PXRD patterns of PE-COF (Figure 2C) strongly aligned with the XRD pattern generated from the AA-eclipsed stacking models, indicating excellent agreement. Conversely, significant disparities were observed when comparing the pattern derived from their corresponding AB' staggered stacking model with the experimental results. The refined unit cell parameters for PE-COF were determined as a = 21.23 Å, b = 21.20 Å, c = 4.37 Å, with $\alpha = \beta = \gamma = 90°$, revealing residuals of Rwp = 3.13% and Rp = 4.27% (Supplementary Materials, Section S5, Figure S8).

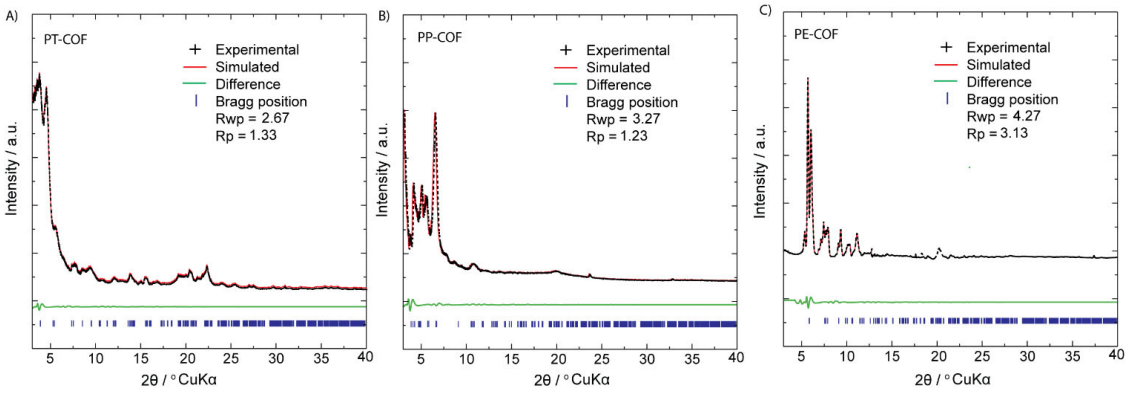

Figure 2. PXRD patterns of A) PT-COF, B) PP-COF and C) PE-COF.

In our investigation, we aimed to assess the chemical and thermal stability of the synthesized PP-COF, PT-COF, and PE-COF for potential practical applications. Our findings revealed that these COFs exhibited exceptional stability, rendering them highly desirable for applications requiring resistance to chemical reactions and elevated temperatures. Through thermogravimetric analysis (TGA), we observed that these COFs demonstrated outstanding thermal stability. Even at high temperatures, they maintained their structural integrity without significant weight loss or decomposition. Notably, these COFs exhibited no signs of breakdown until reaching 400°C in a nitrogen environment. Furthermore, we conducted chemical stability tests on the PP-COF, PT-COF, and PE-COF samples in various solvents at room temperature over a 24-hour period. These solvents included boiling water, ethanol, *N*,*N*-dimethylformamide, dimethylsulfoxide, 3 M HCl at 25°C, and 3 M NaOH at 25°C. Surprisingly, post-testing, the PXRD patterns of the COF samples remained robust and unchanged, indicating the preservation of their remarkable crystallinity even under challenging conditions (Supplementary Materials, Section S6, Figures S9–S11). The study confirms the robust chemical stability of PP-COF, PT-COF, and PE-COF, making them ideal candidates for functionalization. These COFs' appeal as chemically and thermally stable materials is further amplified by their crystalline structure and porous attributes. To facilitate spectroscopic analysis and sensor uses, we grew thin films of PT-COF, PP-COF, and PE-COF on fused silica (Supplementary Materials, Section S4). Despite the susceptibility of imine nitrogen atoms to strong acid protonation, the closely packed 2D COF structures provide stability against hydrolysis, enabling complete and reversible protonation even in humid conditions without notable degradation [13]. To figure out the sensing mechanism of PT-COF, PP-COF and PE-COF toward HCl, we recorded FT-IR spectrum of the sample of PT-COF, PP-COF and PE-COF treated with gaseous HCl (termed PT-COF- HCl, PP-COF- HCl and PE-COF- HCl). Compared with the IR spectrum of pristine PE-COF, PT-COF and PP-COF, the most apparent changes are highlighted in pink where new peaks at approximately 1658,

Preprints (www.preprints.org) | NOT PEER-REVIEWED | Posted: 27 December 2023 doi:10.20944/preprints202312.2004.v1

1660, and 1655 cm^{-1} alongside a reduced intensity in the C=N band (1622-1625 cm^{-1}, Figure 3A–C). These alterations signify the formation of protonated imine bonds ($C=NH^+$), a result of swift protonation of imine nitrogen atoms by HCl gas.

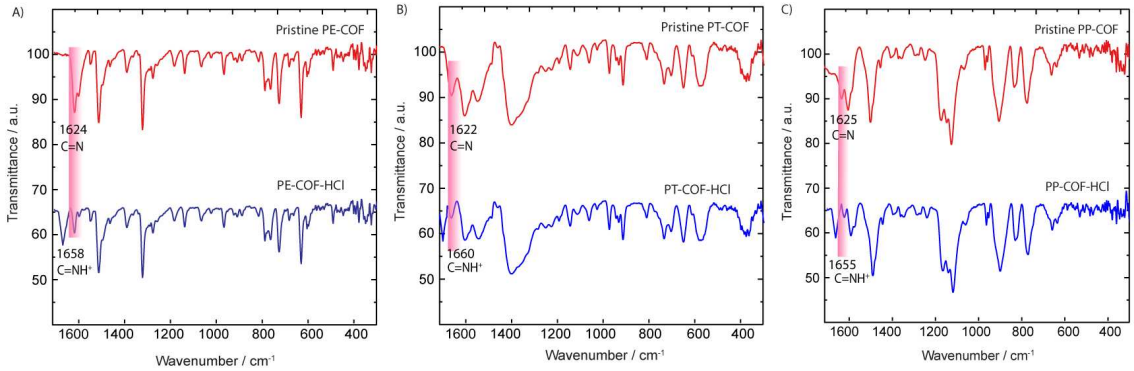

Figure 3. Comparison of the deprotonated and protonated of PT-COF, PP-COF and PE-COF powders.

The photophysical characteristics of our COFs were investigated by analyzing their fluorescence emission spectra in a solution. The COFs were dispersed in 1,4-dioxane at a concentration of 1 mg mL^{-1}, followed by excitation of the suspensions using light at a wavelength of 366 nm. The resulting fluorescence spectra of PT-COF, PE-COF, and PP-COF exhibited emission maxima at 450, 525, and 510 nm, respectively. These distinct emission peaks signify the unique fluorescence behavior inherent in each COF variant. These features encouraged us to investigate the sensing properties of our COFs toward HCl.

Interestingly, upon exposure to HCl gas, suspensions of the PT-COF and PP-COF (1 mg mL^{-1}) in 1,4-dioxane underwent a notable color shift, swiftly transitioning from yellow to dark brown. Subsequent exposure to triethylamine vapor facilitated the rapid restoration of the COF's original yellow color, highlighting the remarkable reversibility inherent in the process of sensing gaseous HCl. Additionally, these color changes were visibly apparent and occurred within response times of less than 1 second—significantly faster than those of previously reported HCl sensors [14]. A video showing the repeated protonation and deprotonation of a pyrene COF film (PP-COF) is supplied in the Supplementary Materials. Similar color transformations were observed in PE-COF from yellow to dark orange upon exposure to HCl vapor demonstrates strong interactions between our synthesized COFs and HCl molecules.

The reversibility of the color change remained uncompromised even after subjecting the COFs to 10 cycles of alternating treatments with HCl and triethylamine (TEA). This endurance underscores the robustness of the COFs in maintaining its reversible properties. Given the distinct and rapid color change perceptible without aid, this porous material stands as a commendable candidate for the detection of HCl gas. To delve deeper into the structural impact of HCl gas followed by TEA gas exposure, the PT-COF, PP-COF, and PE-COF powders underwent analysis using powder X-ray diffraction (XRD) and Fourier-transform infrared spectroscopy (FT-IR). As depicted in (Supplementary Materials, Section S7, Figures S12 and S13), minimal changes were observed in the major peaks of both the powder XRD patterns and IR spectra before and after exposure to HCl/TEA gas. These subtle alterations suggest that the fundamental framework of PT-COF, PP-COF, and PE-COF remained largely intact despite exposure to HCl/TEA gas, indicating their robustness in withstanding chemical exposure without significant structural damage.

The influence of varying HCl concentrations on COF fluorescence was studied using a 1,4-dioxane solution of HCl due to challenges in monitoring gaseous HCl concentrations precisely. Fluorescence spectra of PT-COF, PP-COF, and PE-COF suspensions in 1,4-dioxane revealed distinct responses to different HCl levels (Figure 4). At 1 mmol L^{-1} HCl, fluorescence emission maxima significantly decreased at 450 nm, 525 nm, and 510 nm for PT-COF, PE-COF, and PP-COF, respectively, while new peaks emerged at 540 nm, 625 nm, and 611 nm. These signals vanished at 5

Preprints (www.preprints.org) | NOT PEER-REVIEWED | Posted: 27 December 2023 doi:10.20944/preprints202312.2004.v1

mmol L^{-1} HCl, with subsequent gradual increases from 1 to 50 mmol L^{-1}, showing no further changes in emission. Calibration curves for HCl concentrations (1 to 50 mmol L^{-1}) exhibited linear correlations at 540 nm, 625 nm, and 611 nm, demonstrating detection limits of approximately 17, 10, and 20 nmol L^{-1} for PT-COF, PE-COF, and PP-COF, respectively (Supplementary Materials, Section S7, Figure S14).

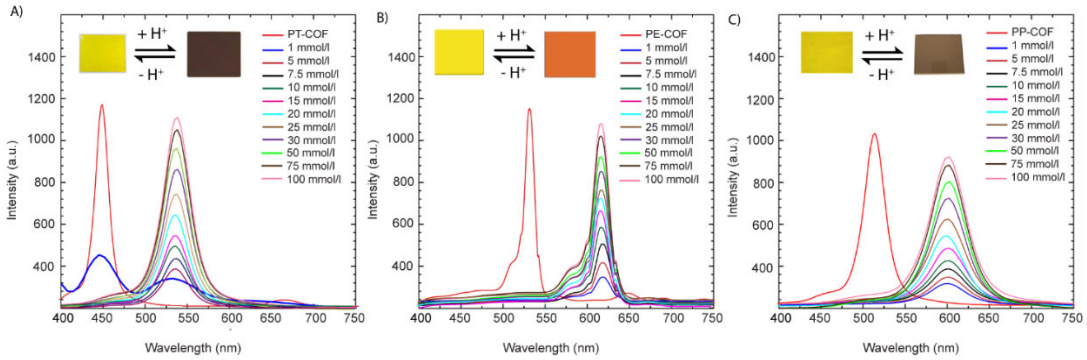

Figure 4. Fluorescence spectra of PT-COF, PE-COF and PP-COF (1 mg/mL) collected from its 1,4-dioxane suspension with different concentrations of HCl (λ_{ex} = 366 nm).

The sensing mechanism of PT-COF, PE-COF, and PP-COF toward HCl involves the probable protonation of imine nitrogen atoms within the COF skeletons when exposed to an HCl atmosphere. This protonation influences the COF's conjugated structure, leading to significant changes in fluorescence emission and color. Unlike many HCl-responsive materials found in literature, where protonation sites typically locate at heteroaromatic nitrogen or amino units, in PT-COF, PP-COF, and PE-COF, the protonation occurs on abundant and periodically distributed imine nitrogen atoms within the imine-linked COF skeletons. As demonstrated by Ascherl et al. [15], the resulting protonated imine ($C{=}NH^+$) groups in COF structures act as stronger electron acceptors than their free imine (C=N) counterparts, accelerating charge transfer towards pyrene units, potentially causing a red-shift in transition photoexcitation energies. Specifically, PE-COF rapidly turned dark orange from yellow when exposed to HCl vapor (Figure 5A), showcasing swift nitrogen atom protonation. Its fluorescence peak shifted from 525 nm to 625 nm with HCl and reverted to 525 nm post-TEA treatment (Figure 5B).

Monitoring pH levels is crucial across various domains like chemistry, environment, and engineering. 2D COFs, containing proton-donating/accepting units, exhibit pH-responsive behaviors driven by nitrogen atom protonation/deprotonation, altering color or fluorescence. These COFs, designed for sensing acid solution pH, also function as effective chemosensors for acidic gases due to their porous structures that allow gaseous analyte diffusion. The pivotal protonation/deprotonation of imine bonds within COFs, influenced by agents like HCl and TEA, significantly affects their electronic properties, crucial for accurate acid sensing in acidic environments.

Preprints (www.preprints.org) | NOT PEER-REVIEWED | Posted: 27 December 2023 doi:10.20944/preprints202312.2004.v1

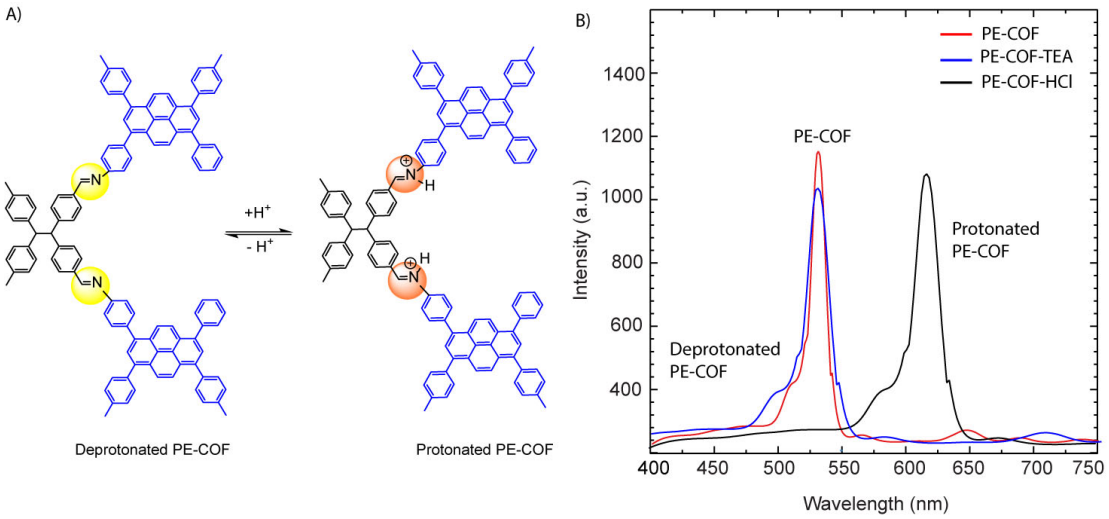

Figure 5. A) Deprotonation, and Protonation Processes within the PE-COF Framework Fluorescent Responses of PE-COF Film; B) Reaction to HCl Gas at 75 mmol/l (λmax = 366 nm); Response to TEA Gas.

We delved into the impact of varying humidity levels on PT-COF, PP-COF, and PE-COF's detection capabilities in the presence of HCl gas. Testing these materials across a spectrum of humidity environments (40%, 50%, 60%, 70%, and 80%) within a controlled Constant Temperature and Humidity Chamber (Supplementary Materials, Section S8, Figure S15) revealed an intriguing outcome. Surprisingly, the fluorescence intensity of PT-COF, PP-COF, and PE-COF remained consistently unaffected by shifts in humidity levels while detecting HCl gas. Even amidst fluctuating humidity conditions, these materials consistently showcased steadfast and robust fluorescence responses. This resilience underscores the stability of their detection capacity, seemingly unswayed by changes in humidity. Further probing into the mechanisms behind this resilience might unveil prospects for deploying these materials in environments characterized by diverse humidity levels, expanding their range of potential applications.

In the exploration of PT-COF, PP-COF, and PE-COF films' reactivity towards co-existing acid gases, our investigation extended to evaluate their responses to CO_2, SO_2, H_2S and Cl_2. As depicted in Figure 6A–C, exposure to CO_2 and SO_2 resulted in no discernible changes in fluorescence intensity within the COF films. However, the presence of H_2S and Cl_2 induced a modest reduction in fluorescence intensity, approximately by ~20%. The discrepancy in fluorescence reduction induced by H_2S and Cl_2 compared to gases like CO_2 and SO_2 may be attributed to their distinct chemical reactivity and interactions with the COF materials. H_2S and Cl_2 exhibit heightened chemical reactivity, with H_2S renowned for its reducing properties and Cl_2 as a potent oxidizing agent. These characteristics likely prompt more substantial chemical interactions with the COF, potentially altering fluorescence intensity. Additionally, H_2S and Cl_2 might possess specific binding affinities or interactions with functional groups within the COF structure, potentially influencing electronic states or modifying emission properties, thereby accentuating the observed decrease in fluorescence intensity. Notably, these findings underscore the COFs' limited reactivity towards certain gases while indicating a moderate interaction with hydrogen sulfide and chlorine gas. Importantly, amidst these varied responses, the COF materials exhibited a distinctive and consistent reactivity to hydrogen chloride (HCl), demonstrating selectivity in detecting this specific acid gas. This observed selectivity emphasizes the potential utility of PT-COF, PP-COF, and PE-COF for targeted and precise detection of hydrogen chloride, elucidating their applicability in scenarios where specific gas identification is paramount.

Additionally, acknowledging the significance of volatile organic compounds (VOCs) as potential interference gases in certain contexts, we scrutinized the impact of four distinct VOCs (benzene (C_6H_6), toluene (C_7H_8), xylene (C_8H_{10}), and dichloromethane (CH_2Cl_2)) on the detection

Preprints (www.preprints.org) | NOT PEER-REVIEWED | Posted: 27 December 2023 doi:10.20944/preprints202312.2004.v1

capabilities of hydrogen chloride gas by PT-COF, PP-COF, and PE-COF. As illustrated in Figure 6D,F, exposure to these VOCs did not prompt noticeable alterations in fluorescence intensity. The lack of noticeable changes in COF fluorescence when exposed to benzene, toluene, xylene, and dichloromethane suggests these VOCs have limited interaction with the COF structure. This suggests a relatively stable response of the PT-COF, PP-COF, and PE-COF materials in the presence of these specific VOCs, underscoring their potential efficacy for precise detection of hydrogen chloride gas despite the coexistence of certain interfering gases.

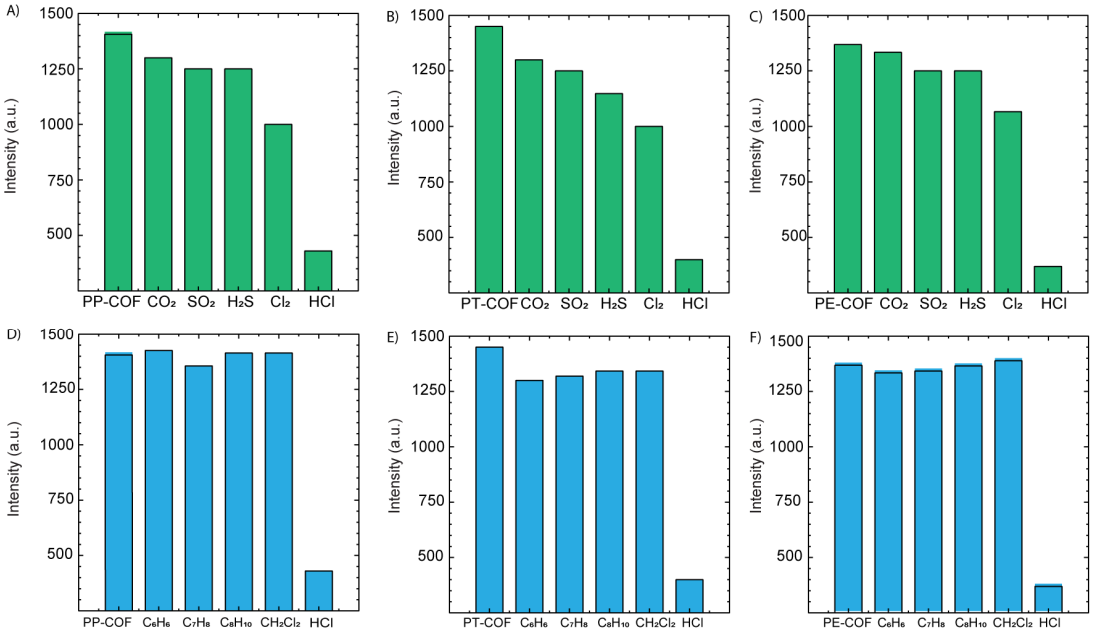

Figure 6. PP-COF, PT-COF, and PE-COF Films Responses to Other Potential Co-existing Interference Gases: (A-C) Acid Gases; (D-E) Volatile Organic Compounds.

Additionally, we evaluated the selectivity of PT-COF, PP-COF, and PE-COF towards HCl by introducing various acids at a concentration of 20 mmol L^{-1} to the suspension solutions of PT-COF, PP-COF, and PE-COF. (Supplementary Materials, Section S9, Figure S16) demonstrates that solely HCl induced a notable red-shift in the fluorescence emission peaks of the PT-COF, PP-COF, and PE-COF to 540, 625 and 611 nm, respectively, accompanied by remarkably intense fluorescence emissions. The COFs functions as a sensor with a strong fluorescence shift in the following order: HCl > HBr > H_2SO_4 > HNO_3 > H_3PO_4 > CH_3COOH. The order of the fluorescence shift in the COFs sensors toward different acids could be attributed to the varying strengths of the acids and their interactions with the COF's structure. The trend might correlate with the acids' abilities to protonate the COF's functional groups, inducing changes in its electronic structure and consequently affecting its fluorescence properties. Stronger acids like HCl are more likely to readily donate protons, causing significant alterations in the COF's electronic configuration, leading to more pronounced fluorescence shifts compared to weaker acids like acetic acid (CH_3COOH), which have comparatively lower proton-donating capabilities and may induce lesser changes in the COF's structure and fluorescence characteristics.

3. Conclusions

In conclusion, the synthesis of stable fluorescence COFs—PT-COF, PP-COF, and PE-COF—via distinct polycondensation reactions demonstrates their structural diversity and robust chemical compositions, verified through FTIR analysis. These COFs exhibit exceptional characteristics: high crystallinity, impressive thermal stability up to 400°C, and remarkable surface areas spanning 730-1098 m^2 g^{-1} as determined by PXRD and BET analyses. The developed COF-based chemosensor

showcases rapid and sensitive detection of gaseous HCl, manifesting significant color and fluorescence changes, reversible upon exposure to TEA vapor. Notably, the sensor's recovery post-exposure to TEA vapor accentuates its remarkable reversibility. This study presents COFs as promising platforms for responsive sensing applications, particularly in detecting toxic gases, marking an innovative direction in utilizing COFs for advanced air quality monitoring devices.

Supplementary Materials: The following supporting information can be downloaded at the website of this paper posted on Preprints.org.

Acknowledgments: The Research Affairs Sector of UAE University (grant number. G00004310) is gratefully acknowledged by the authors as providing substantial financial assistance.

Conflicts of Interest: There are no competing interests declared by the authors.

References

1. Kelly: F.J., & Fussell, J.C. (2015). Air pollution and public health: emerging hazards and improved understanding of risk. Environmental Geochemistry and Health, 37(4), 631-649. DOI: 10.1007/s10653-015-9720-1
2. Lelieveld, J., et al. (2015). The contribution of outdoor air pollution sources to premature mortality on a global scale. Nature, 525(7569), 367-371. DOI: 10.1038/nature15371
3. Muthukumar, P., & John, S.A. (2011). Highly sensitive detection of HCl gas using a thin film of meso-tetra(4-pyridyl)porphyrin coated glass slide by optochemical method. Sensors and Actuators B: Chemical, 159(1), 238-244. doi.org/10.1016/j.snb.2011.06.079
4. Nakagawa, K., et al. (2000). HCl gas sensing properties of TPPH2 dispersed in various copolymers. Sensors and Actuators B: Chemical, 65, 138-140. doi.org/10.1016/S0925-4005(99)00469-4
5. Baron, M.G., Narayanaswamy, R., & Thorpe, S.C. (1996). Hydrophobic membrane sensors for the optical determination of hydrogen chloride gas. Sensors and Actuators B: Chemical, 34(1), 511-515. doi.org/10.1016/S0925-4005(96)01942-9.
6. Onyancha, R.B., et al. (2021). A systematic review on the detection and monitoring of toxic gases using carbon nanotube-based biosensors. Sensing and Bio-Sensing Research, 34, 100463. doi.org/10.1016/j.sbsr.2021.100463
7. Dalaijamts, C., et al. (2021). Quantitative characterization of population-wide tissue- and metabolite-specific variability in perchloroethylene toxicokinetics in male mice. Toxicological Sciences, 182(2), 168-182. doi: 10.1093/toxsci/kfab057.
8. Zhang, C., et al. (2019). Flexible and transparent microwave–infrared bistealth structure. Advanced Materials Technologies, 4(8), 1900063. doi.org/10.1002/admt.201900063.
9. Yin, M., Yu, L., & Liu, S. (2017). Synthesis of thickness-controlled cuboid WO3 nanosheets and their exposed facets-dependent acetone sensing properties. Journal of Alloys and Compounds, 696, 490-497. doi.org/10.1016/j.jallcom.2016.11.149.
10. Huang, L., et al. (2016). Electrical gas sensors based on structured organic ultra-thin films and nanocrystals on solid state substrates. Nanoscale Horizons, 1(5), 383-393. DOI:10.1039/C6NH00040A
11. Lohse, M.S., & Bein, T. (2018). Covalent organic frameworks: Structures, synthesis, and applications. Advanced Functional Materials, 28(33), 1705553. DOI:10.1002/adfm.201705553.
12. Chung, W.-T., et al. (2023). Recent advances in metal/covalent organic frameworks based materials: Their synthesis, structure design and potential applications for hydrogen production. Coordination Chemistry Reviews, 483, 215066. DOI:10.1016/j.ccr.2023.215066.
13. Qian, Y., et al. (2022). Fluorescent covalent organic frameworks: A promising material platform for explosive sensing. Front Chem, 10, 943813. doi: 10.3389/fchem.2022.943813.
14. EL-Mahdy, A.F.M., et al. (2020). Dual-function fluorescent covalent organic frameworks: HCl sensing and photocatalytic H2 evolution from water. Advanced Optical Materials, 8(18), 2000641. doi.org/10.1002/adom.202000641.
15. Ascherl, L., Evans, E. W., Gorman, J., Orsborne, S., Bessinger, D., Bein, T., Friend, R. H., & Auras, F. (2019). Perylene-Based Covalent Organic Frameworks for Acid Vapor Sensing. Journal of the American Chemical Society, 141(39), 15693-15699. DOI: 10.1021/jacs.9b08079.

 doi:10.20944/preprints202312.2004.v1